Available online at www.sciencedirect.com
SCIENCE DIRECT®
Journal of Chromatography B, 818 (2005) 89–97
JOURNAL OF CHROMATOGRAPHY B
www.elsevier.com/locate/chromb

The use of confocal laser scanning microscopy to study the transport of biomacromolecules in a macroporous support

Anuradha Subramanian[a,*], Jennifer Hommerding[b]

[a] *Department of Chemical Engineering, University of Nebraska, 207L Othmer Hall, Lincoln, NE 68588-0463, USA*
[b] *Department of Biosystems and Agricultural Engineering, University of Minnesota, 1390 Eckles Ave., St. Paul, MN 55108, USA*

Received 12 July 2004; accepted 5 October 2004
Available online 15 January 2005

Abstract

Large-pore materials or supports resembling polymer conduits are used as packing material in chromatographic operations. Our ongoing research has shown that, when modified with peptides or ligands, chitosan beads that are 800 μm in diameter and have 3.5% solids can be used as matrices in bioseparations. The goal of the present study is to evaluate the transport properties of biomolecules in the modified chitosan beaded matrices. Batch uptake experiments with fluorescently tagged pure human IgG, human IgA and human IgM were conducted to visualize the distribution of binding sites throughout the bead as well as to evaluate restrictions to diffusion, if any, within the support. The chromatographic performance of the macrobeads was first assessed by the classical height equivalent of a theoretical plate HETP analysis. The independence of HETP on linear flow rates studied suggests that a likely mode of solute transport within the macrobeads may be a combination of convection and diffusion-convective components. By using fluorescent-tagged immunoglobulins, the penetration of the adsorbent particle at different times and different levels of saturation was visually observed. The profiles obtained from dynamic experiments were compared to the profiles obtained from finite bath experiments. With an increase in the incubation time, the degree of penetration increased and the bead interior was saturated with FITC immunoglobulins at the end point of the finite bath experiment. In the dynamic uptake experiment, the degree of penetration was found to be a function of the linear velocity and level of breakthrough. The penetration of the bead radius, at times lower than the predicted diffusion time, suggests that the mode of transport in the chitosan beads is governed by a combination of convective and diffusive forces.

Keywords: Protein transport; Biomolecules; Convection; Confocal microscopy; Diffusion; FITC

1. Introduction

Optimal design of supports used in process-scale chromatography requires a balance among separation factors, such as binding capacity and operational flow rates with minimal operational times [1]. Flow-through or perfusion chromatography contrasts with conventional liquid chromatography in that diffusivity in these supports is augmented by convection. By utilizing a convective component of mass transport, flow-through chromatography reduces retention time of the sample while maintaining resolution and high throughputs.

Mathematical models are most frequently used to describe the dynamics of adsorption of protein-ligand interactions. Kinetics models are used to predict the parameters that characterize the intraparticle mass transfer mechanisms. Several investigators have approached the prediction of transport rates using the plate height method to account for the combined effects of convection and diffusion [2–5]. Although these approaches have shown to be effective in predicting the effects of transport in particular chromatographic environments, these models present limitations. For example, the model developed elsewhere [4] is restricted to the case of linear equilibrium, where the adsorption and desorption kinetics

* Corresponding author. Tel.: +1 402 472 3463; fax: +1 402 472 6989.
E-mail address: asubramanian2@unl.edu (A. Subramanian).

1570-0232/$ – see front matter © 2004 Elsevier B.V. All rights reserved.
doi:10.1016/j.jchromb.2004.10.014

are rapid and the intraparticle flow field is uniform. This is not always the case in chromatographic applications. Additionally, estimates of apparent diffusivities are based on intraparticle diffusion models such as pore diffusion or surface diffusion. These models are not always accurate for varying solvent conditions. Despite the fact that these models are useful predictive methods of chromatographic systems, direct measurements of the adsorption of proteins on supports could be an invaluable tool for the complex tasks of design, optimization and scale-up of adsorption processes.

The fluid velocities in porous agarose beads were first observed directly in their natural environment, a packed chromatographic bed [5]. In a previous study, a microtome was used to section fluorescently labeled beads to evaluate the effects of antibody density on a support's efficiency [6]. Several groups of researchers have used confocal laser scanning microscopy (CLSM) to measure the uptake of dyes and proteins on individual particles under varying binding conditions [7–11]. Using CLSM, it is possible to obtain three-dimensional images of individual chromatographic support particles that directly illustrate the amount of protein uptake. These studies will provide a fundamental understanding of protein transport mechanisms in chromatography, which can serve as a template for the optimization of chromatographic support design.

We are interested in the fabrication of hydrogel beads with a macroporous open architecture (Fig. 1) and evaluation of its utility in chromatographic bioseparations. In our present study we have chosen chitosan as the natural polymer for hydrogel preparation, as it provides a primary amino group facile substitution and modification. We have documented the use of modified chitosan beads in the separation of immunoglobulins from biological mixtures elsewhere [14,15]. The goal of this study is to understand the protein transport mechanisms thorough direct measurement of intraparticle concentration profiles in the hydrogel beads prepared in our laboratories, using confocal microscopy.

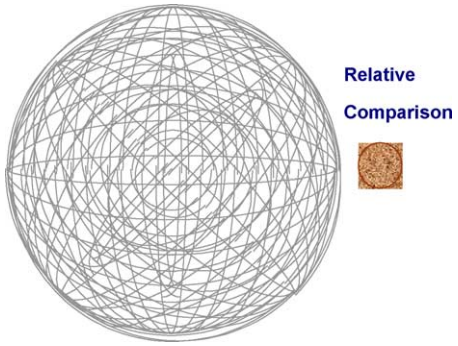

Fig. 1. Schematic of bead size and bead structure comparison. Chitosan beads used in this study possess a nominal diameter of 600–800 μm and a solid content of 3.5%. The chitosan hydrogel beads employed in this study are 5–20 times larger than conventional small, high surface beads.

2. Materials and methods

Lyophilized, 95% pure human IgG, lyophilized human serum albumin, human serum, fluorescein isothiocyanate (FITC) labeled hIgG, were purchased from Sigma Co. (St. Louis, MO). FITC conjugated hIgA, FITC conjugated hIgM were purchased from Jackson ImmunoResearch (West Grove, PA). Immunoaffinity separations were performed with a Spectra/Chrom LC column (1.77 cm^2/cm), an Amersham-Biosciences HR 5/5 column (0.5 cm i.d.), an Amersham-Biosciences C 10/20 column (1 cm i.d.) (Piscataway, NJ), a Cole Parmer Materflex peristaltic pump (Niles, IL), a Spectronic spectrophotometer (Rochester, NY), and a BioRad UV monitor (Hercules, CA) was used to monitor chromatography from Fisher Scientific (Itasca, IL).

2.1. Ligand modified chitosan beads

The preparation and modification of chitosan beads with a carboxyethyl group containing anionic ligand is presented in detail elsewhere [12]. Briefly, the beads were first reacted with a bifunctional epoxide (1,4 butenediol) to install a four carbon spacer arm and a terminal reactive epoxide (oxirane) moiety. In a second step, the reactive epoxide groups were titrated with an aqueous solution of carboxyethyl group containing anionic ligand as detailed elsewhere [12]. The chitosan beads used in this study had a nominal diameter of 800 μm and a solids content of 3.5%, which was determined by thermogravitametric analysis. Ligochem Inc.™ provided the carboxyethyl group containing anionic ligand modified chitosan beads (LMCB) as a generous gift [12].

2.2. Porosity determination

Pulse injections of 1 ml were made with blue dextran at a concentration of 0.5 mg/ml to estimate the packed bed or interstitial porosity under unretained conditions (i.e. dissolved in 1 M NaCl buffer). Blue Dextran was detected at 640 nm using the online spectrophotometer. To determine the intraparticle porosity, sodium nitrate at a concentration of 0.01 M was pulsed into the system. Sodium nitrate was monitored at 310 nm by the online spectrophotometer. Interstitial porosity (ε) was determined from the first moments obtained under various flow rates using blue dextran by using equation listed below, there after the intra-particle porosity was determined from the first moment data obtained from pulse injection of sodium nitrate. The porosity of the column is related to the first moment and linear velocity as:

$$\mu_1 = \frac{L}{u}(\varepsilon_i + (1 - \varepsilon_i)\varepsilon_p b_0),$$

where b_0 equals 1.0 under unretained conditions.

2.3. HETP analysis and calculations

LMCB beads were packed in 8.5 cm × 1.0 cm (i.d.) cm column obtained from Amersham-Biosciences. The chro-

matographic system was an LC system with a spectroflow 783 detector at 280 nm and a peristaltic masterflex pump from Cole Parmer (Apple Valley, MN). The absorbance data from the detector was saved onto a desktop computer in Microsoft Excel format via a laboratory-built interface module. Column plate heights with hIgG were determined by applying a 15 mg pulse of hIgG at varying linear velocities through a Pharmacia column (1.0 cm diameter × 8.5 cm length) under non-retaining conditions by using a loading buffer containing 0.5 M NaCl. The raw chromatographic data was imported into a MATLAB routine. The elution profiles obtained were approximated with a Gaussian profile and the first and second moments were determined. The total HETP of the Gaussian profile was determined using the following equation:

$$H_{\text{tot}} = \frac{L}{5.54}\left(\frac{t_{\text{w},1/2}}{t_{\text{r}}}\right)^2,$$

where $t_{\text{w},1/2}$ is the width of the Gaussian profile at half-height and t_{r} is the retention time.

2.4. FITC conjugated hIgG batch experiments

Twelve test tubes were prepared in the following manner. First, 100 μl of water was pipetted into 1.5 ml microcentrifuge tubes and the volume level was marked. Then approximately 200 μl of a 50% (v/v) slurry of LMCB were transferred into the microcentrifuge tubes to yield approximately 100 μl of beads. The beads were allowed to settle for at least 5 min and then adjusted to ensure the appropriate volume level of 100 μl. The liquid overlay was then pipetted off. The FITC conjugated hIgG solution was diluted in a binding buffer (10 mM KH_2PO_4, pH 6.0) to make a 3.75 mg/ml FITC conjugate hIgG solution. 300 μl of this solution was pipetted into all 12 test tubes, which were wrapped with foil to provide a dark environment. The tubes were placed on an end-to-end rotator and allowed to rotate for 24 h at 4 °C. The reaction was stopped at various times by removing the supernatant, which was stored for analysis of fluid phase protein concentration. The beads were then resuspended in 1.25 ml of the buffer to properly wash the beads of the FITC solution, and the wash removed for protein analysis. This cycle was repeated twice. Beads were stored at 4 °C in binding buffer until analyzed by confocal microscopy. The procedure was conducted at 2, 10, 30, 60, 120, 240 min intervals and at 24 h. All experiments were conducted in duplicate. Similar experiments were conducted for hIgG-FITC feed concentrations of 10 and 0.5 mg/ml. Additionally, similar experiments were conducted with FITC conjugated hIgA and hIgM. Two test tubes were prepared as described above, yielding approximately 50 μl of beads. The liquid overlay was then pipetted off. 95 μl of a 2 mg/ml solution of FITC-hIgA or FITC-hIgM were added to the tubes along with 475 μl of binding buffer. Tubes were wrapped with foil to provide a dark environment, placed on an end-to-end rotator and allowed to rotate for 24 h at 4 °C. The reaction was stopped by removing the supernatant. The beads were resuspended in 1.25 ml of the respective buffer (10 mM KH_2PO_4, pH 6.0) to properly wash the beads of the FITC solution, and the wash was then removed for protein analysis. This cycle was repeated twice. Beads were stored at 4 °C in a binding buffer until analyzed by confocal microscopy. Prior to confocal analysis the beads were sliced in half at the midpoint with a small surgical razor blade under a laboratory microscope. This was done so that section scanning could be conducted at the midpoint of the bead while minimizing optical effects due to adsorption and light scattering.

2.5. Confocal analysis

FITC prepared samples were viewed using a BioRad MRC-1024 confocal microscope. This microscope was attached to a Nikon Diaphot inverted microscope (BioRad Labs. Hercules, CA) equipped with a 15 mW Krypton/Argon laser and FITC (excitation filter 470–490) filter sets. Individual beads were analyzed by horizontal scanning (section scanning). As a control, unlabeled beads were scanned and the background of fluorescence was found to be negligible. The samples were viewed using a 10×, 0.30 plan fluor objective. The image size for all images was 512 × 512 pixels. Digital images were collected using a Compaq ProSignia model 300 personal computer with LaserSharp version 3.2 software. Digital images were stored on an Iomega Jaz drive for future analysis using NIH Image version 1.62.

2.6. FITC conjugated hIgG dynamic experiments

For this experiment, a Amersham-Biosciences HR 5/5 column (3.5 cm × 0.5 cm i.d.) was filled with 0.7 ml of LMCB beads and wrapped in foil to provide a dark environment. The column was equilibrated with a binding buffer (10 mM KH_2PO_4, pH 6.0). A protein solution of 10 mg/ml FITC-hIgG diluted in the same buffer was continuously fed to the column at a linear velocity of 9.0 cm/min until the absorbance of the effluent at 280 nm reached approximately 90% of the feed concentration. A similar experiment was conducted using a 2:1 FITC-hIgG to pure hIgG 10 mg/ml solution in binding buffer, which was fed continuously to the column until the column effluent reached approximately 90% of the feed concentration. The column was then washed with the binding buffer until the absorbance of the effluent at 280 nm reached zero. Approximate binding capacity values were determined by making a material balance between the mass of protein feed and the mass of protein in the fall-through based on 100% protein recovery. After each column was washed, the column matrix was emptied into a 5 ml plastic test tube and covered with foil. The test tubes were stored at 4 °C until analyzed by confocal microscopy as described above in the FITC batch methods.

3. Results and discussion

There is a need to develop chromatographic supports that can significantly reduce processing times and provide mechanical and chemical stability, low pressure drop characteristics and good fluid-flow properties. To enhance the rate of separation, efforts have been focused on creating non-porous particles with a high surface area to volume ratio and on creating supports that encourage convective mass transfer [13]. Non-porous particles eliminate the limitations imposed by intraparticle mass transfer, but the small size of these particles induces process constraints in terms of huge pressure drops across chromatographic columns. For porous supports in preparative chromatography, the support matrix should meet the requirements of rapid transfer of solute (i.e. protein in feed) to binding sites on bead and high available particle surface area to enable a high total binding capacity per unit volume of adsorbent bed.

We are interested in the design and development of supports and surfaces based on natural polymers like chitosan, modified starch and alginate for use in biomaterial and biomedical applications. In particular, we are interested in the development of novel surfaces and surface chemistries based on chitosan as the background polymer. As part of our ongoing research, we have evaluated the chromatographic performance of LMCB and the results are presented elsewhere [14,15]. Briefly, LMCB was shown to specifically interact with immunoglobulins over other serum proteins like albumin and fibrinogen. In this study we chose FITC tagged immunoglobulins as the biomolecules of interest. The focus of this research paper is to understand the transport mechanism of solute biomolecules like Ig's through macroporous supports. In this study we have used chitosan-based hydrogel beads (3.5% solids content and 800 μm in diameter) which resemble a scaffold of polymeric networks (Fig. 1). The matrix architecture of chitosan beads used in this study is different from all other liquid chromatography bio-separation matrices. The matrices used in this study are beads with large diameter; low solid content, low density chitosan constructs which permit homogeneous ligand utilization throughout the bead interior. This is in contrast to the small diameter, high density, high surface area beads with intricate pore-based architecture.

First, the chromatographic performance of LMCB was evaluated by classical HETP analysis. Plate heights were measured from chromatograms of IgG (M_r = 150 kDa). Application of IgG pulses produced asymmetric peaks at lower flow rates. Fig. 2B compares the experimental plate heights obtained for the IgG pulses with calculated plate heights by the modified van Deemter equation for packings showing forced convective solute transport (Fig. 2A) [16]. At linear velocities greater than 3 cm/min, the plate height is independent of linear velocity, as can be seen in Fig. 2B. This behavior can be attributed to features of diffusion-convective supports. As a comparison, HETP analysis of classical support, zirconia beads with a particle diameter of 25 μm and a pore size of 22 nm, is shown in Fig. 2C. The elution profiles obtained with injections of sodium nitrate were approximated with a Gaussian profile using a MATLAB subroutine and the first and second moments were determined. The intraparticle porosity was estimated to be 0.9 and this was found to be in agreement with values reported in literature [13,19]. This is not surprising as the hydrogel beads used in this study are 4.25% solids.

The independence of HETP on linear flow rates studied suggests that solute transport within LMCB may involve a combination of convection and diffusion-convective components. We seek to better understand and elucidate the mode of transport within these beads by visualizing the access of the bead interior with fluorescently tagged hIgG molecules in a dynamic-mode. We hypothesize that if the mechanism of solute transport in LMCB is aided by convective fluxes, then at bead contacting times [(t_b, where $t_b = (d_b/u)$] that are far less than the time for diffusion [(t_D, where $t_D = R_p^2\varepsilon_p/5D$] of

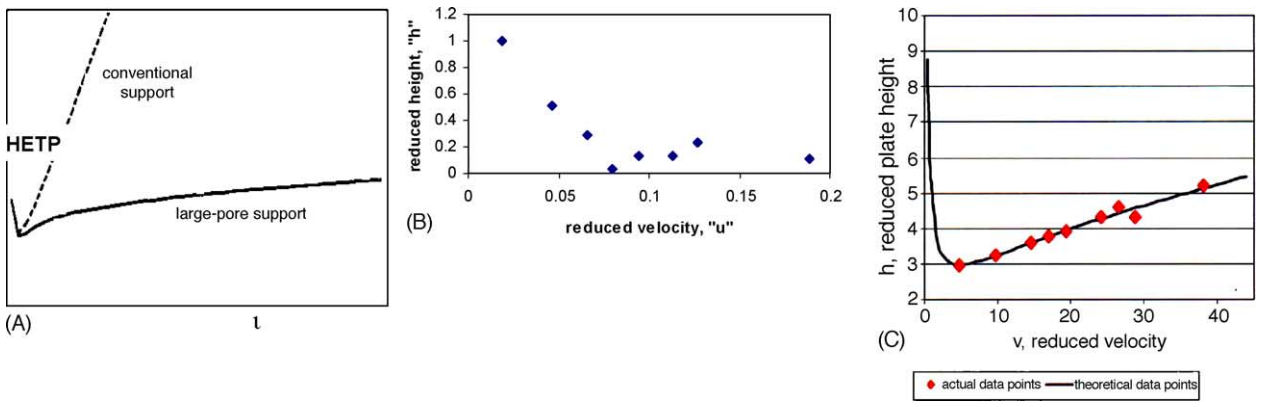

Fig. 2. (A) Effect of intraparticle convection on the HETP of a column obtained by a modified van Deemter equation (adapted from [16]). Dotted line shows plate heights for a conventional support whereas the solid line shows plate height values for large-pore supports. (B) Plate heights for hIgG on LMCB under non-retaining conditions. Column plate heights with protein solutes were determined by applying a 15 mg pulse of hIgG at varying linear velocities through a Pharmacia column (1.0 cm × 8.5 cm). Plate heights were predicted as described in the methods section. (C) Plate heights for lysozyme on EDTPA modified zirconia beads, 25 μm in diameter and pore size of 22 nm. Data adapted from [20].

the solute within the bead, one should visualize fluorescent stain within the bead radius. As the beads under investigation are 3.5% solids, we can assume that they provide an aqueous environment for solute transport. The extent to which stain is visible within the bead interior can be taken as a qualitative measure of the strength of convective forces over diffusive or diffusive-convective forces.

Prior to a complete analysis of the mechanism of solute transport, it is useful to determine the layout of binding sites within the support. The distribution of binding sites was visualized by immobilizing fluorescent antibodies (IgG, IgA and IgM) to sites under batch binding conditions. To better understand the distribution of binding sites within the macroporous LMCB, confocal microscopy analysis using horizontal section scanning of individual beads was performed. FITC labeled hIgG was bound to LMCB beads in an equilibrium batch experiment. Samples of the beads at defined times were taken and the hIgG distribution visualized by measuring the fluorescence profile along the diameter of the bead in a 25 μm deep section below the midpoint. By taking samples at various time points for three independent feed concentrations (C_o), the progression of protein uptake could be visualized. Fig. 3 shows a series of scanning images for the adsorption of hIgG to LMCB beads for feed concentrations [C_o] of 0.5, 3.75 and 10 mg/ml and with hIgG binding capacities of 1.5, 9.75 and 32 mg of hIgG/ml of beads, respectively. The amount of hIgG adsorption increases with increasing concentration, as expressed by the penetration of FITC labeled hIgG in the internal portions of the bead. Additionally, the amount of hIgG penetration into the bead also varies with respect to time. Figs. 4–6 show the respective translation into a series of normalized fluorescence profiles. The increased area below the curves shows an increase in hIgG penetration with increasing concentration. Additionally, Fig. 7 shows the intensity profiles from hIgA and hIgM for a batch equilibrium binding experiment. The profiles indicate that, with sufficient feed concentration, both hIgA and hIgM have diffused throughout the entire bead cross-section.

Image analysis of individual beads by confocal microscopy, shown graphically by the intensity profiles, indi-

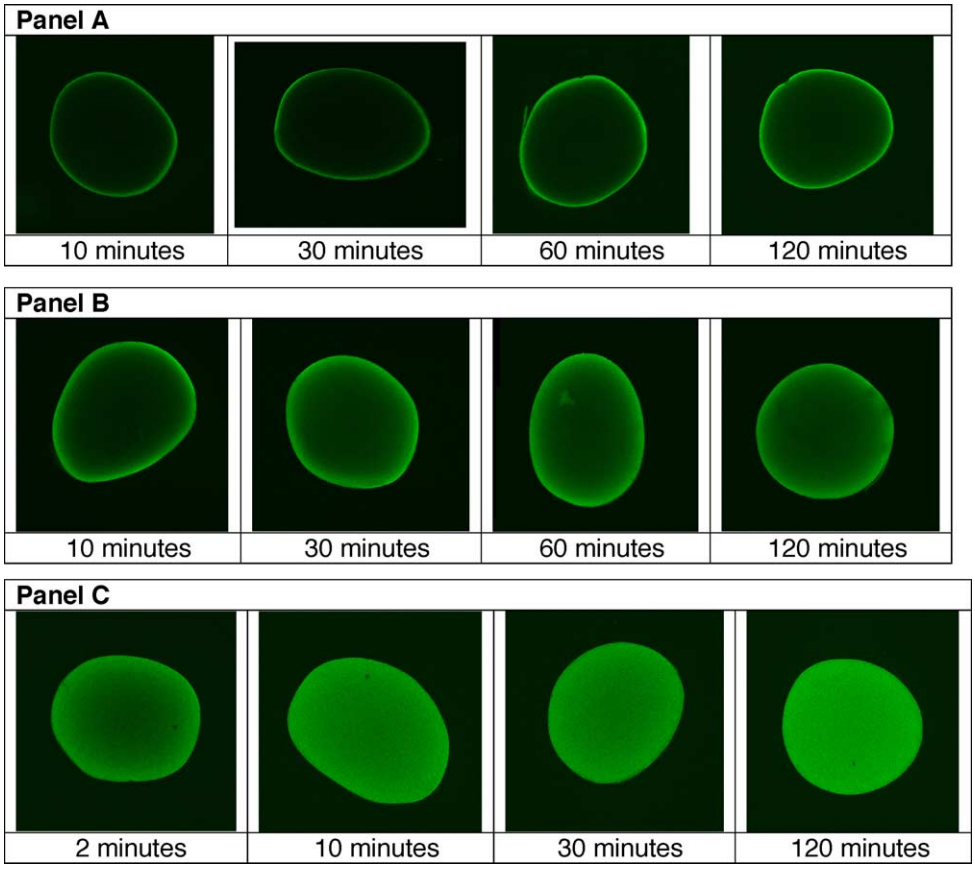

Fig. 3. Confocal images of sample chitosan beads (LMCB) from batch uptake of hIgG. LMCB were incubated with hIgG-FITC in a static mode and upon completion of the binding step the beads were washed copiously with a low salt wash buffer. The beads were then sectioned and viewed under a confocal microscope. Panel A depicts the confocal images obtained when the beads were incubated with hIgG-FITC at a feed concentration (C_o) of 0.5 mg/ml. Panel B depicts the confocal images obtained when the beads were incubated with hIgG-FITC at a feed concentration (C_o) of 3.75 mg/ml. Panel C depicts the confocal images obtained when the beads were incubated with hIgG-FITC at a feed concentration (C_o) of 10.0 mg/ml. The corresponding to binding capacities [Q_x] in panels A, B and C are 1.5, 9.75 and 32 mg hIgG/ml of beads, respectively. Samples were taken at defined times as shown. Images were obtained by taking a 25 μm deep z-section scan at the midpoint of the bead.

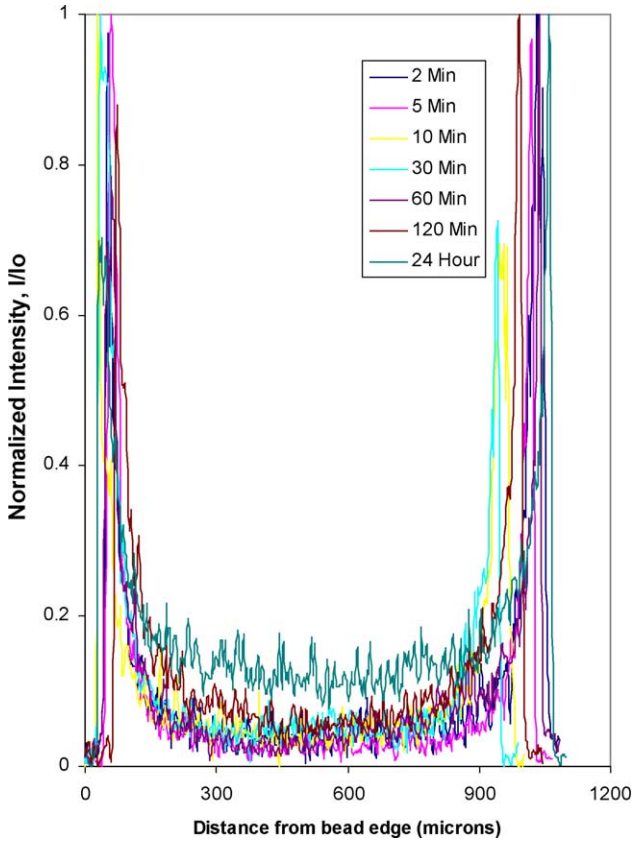

Fig. 4. Normalized fluorescence intensity profile (I/I_0) vs. bead radius. LMCB were incubated with labeled hIgG at feed concentration of 0.5 mg/ml FITC-hIgG in a batch mode. The coupling step was stopped at various incubation times, beads were washed and beads were scanned by confocal microscopy. Binding capacity was calculated to be 1.5 mg FITC-hIgG/ml bead. Normalized intensity plots correspond with images on panel A in Fig. 3.

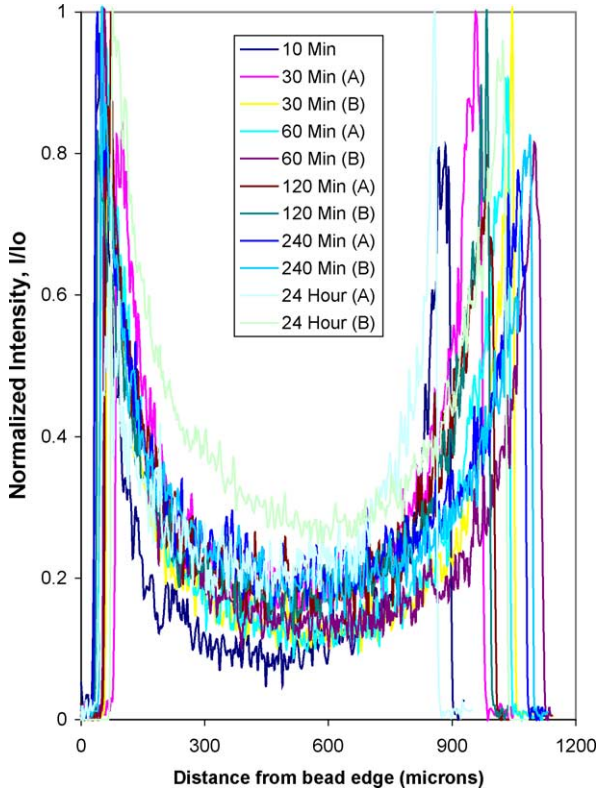

Fig. 5. Normalized fluorescence intensity profile (I/I_0) vs. bead radius. LMCB were incubated with labeled hIgG at feed concentration of 3.75 mg/ml FITC-hIgG in a batch mode. The coupling step was stopped at various incubation times, beads were washed and beads were scanned by confocal microscopy. Binding capacity was calculated to be 9.6 mg FITC-hIgG/ml bead. Normalized intensity plots correspond with images on panel B in Fig. 3.

cates that fluorescently tagged Ig molecules were distributed throughout the entire support cross-section. Thus, it appears that for molecules as large as IgM (M_r = 900 kDa) there are no apparent steric hindrances to encumber diffusional transport to the interior of the bead, and binding sites are distributed throughout the bead.

3.1. Dynamic FITC labeling

To determine the mode of mass transport within LMCB, uptake experiments were conducted in column-mode using a 10 mg/ml protein feed solution at linear velocities of 1.1 and 9.0 cm/min. These experiments were conducted in a chromatographic column packed with LMCB beads, which provides for the analysis of hIgG uptake in a natural purification setting. Fig. 8 shows a series of horizontal scanning images for the adsorption of hIgG to LMCB beads for the two linear velocities. The first set of images represents hIgG uptake for a feed concentration of 10 mg/ml where the column was fed continuously until the outlet concentration reached approximately 90% of the feed concentration at a linear velocity of 9.0 cm/min. The loading step of the column operation required a total of 2.78 min and the wash step was conducted at the same velocity. In most experiments conducted under these conditions, the signal returned to baseline in less than a minute. The second set of images represents hIgG uptake for a feed concentration of 10 mg/ml, where the column was fed continuously until the outlet concentration reached approximately 90% of the feed concentration at a linear velocity of 1.1 cm/min. Figs. 9 and 10 show the corresponding intensity profiles of LMCB beads across the particle diameter. Fig. 10 shows the intensity profile for a linear velocity of 9.0 cm/min. At the midpoint of the bead (the measured radius of the bead equal to 1.0 of the entire bead radius, $r = 1.0R$), over 50–65% of the sites available were saturated as determined by the normalized intensity ratio I/I_0. At $r = 0.5R$, 70% (i.e. $I/I_0 = 0.7$) of the sites available were saturated and at $r = 0.25R$ approximately 80% (i.e. $I/I_0 = 0.8$) of available sites were saturated. Fig. 9 shows the intensity profile for a linear velocity of 1.1 cm/min. The profile indicates that hIgG penetrated throughout the entire bead cross-section at a near 100% saturation.

Table 1 provides calculated times of diffusion of hIgG within an 800 μm bead and also provides the bead contacting times at the linear velocities used in this study. We assume that

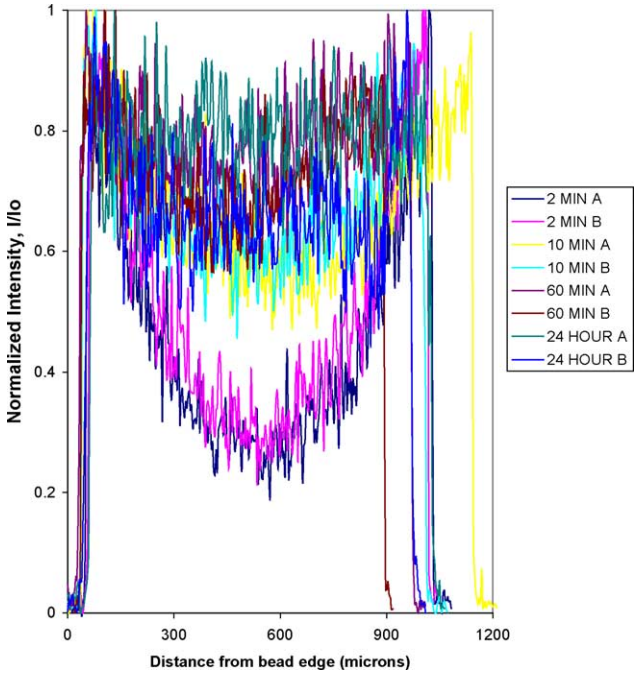

Fig. 6. Normalized fluorescence intensity profile (I/I_0) vs. bead radius. LMCB were incubated with labeled hIgG at feed concentration of 10.0 mg/ml FITC-hIgG in a batch mode. The coupling step was stopped at various incubation times, beads were washed and beads were scanned by confocal microscopy. Binding capacity was calculated to be 32.0 mg FITC-hIgG/ml bead. Normalized intensity plots correspond with images on panel C in Fig. 3.

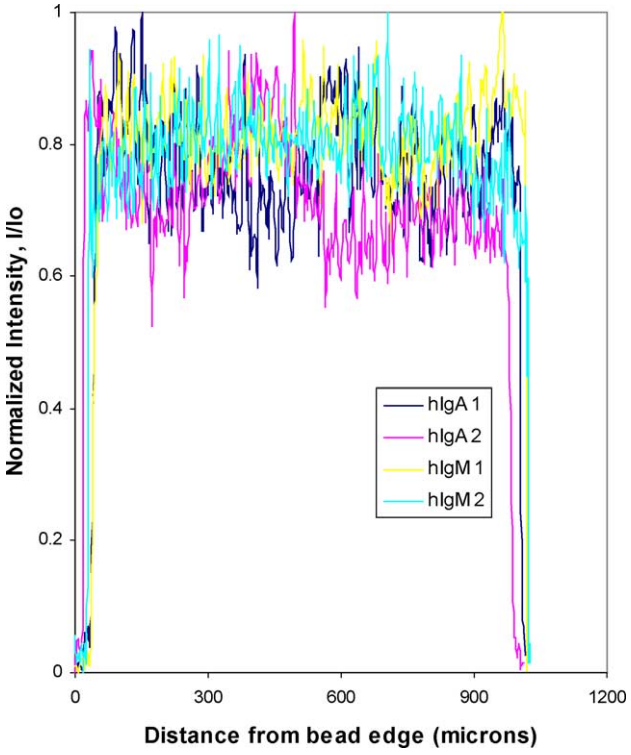

Fig. 7. Fluorescence intensity profile for uptake of hIgA-FITC and hIgM-FITC on LMCB in batch mode. LMCB were incubated with hIgA-FITC for 24 h and upon completion of the binding step the supernatant was removed and the beads were washed. The beads were viewed under a confocal microscope. Four independent beads were scanned and two representative scans are shown. A similar but independent experiment was conducted with hIgM-FITC.

under low-salt or binding conditions the coupling between the IgG molecule and site on the chitosan bead is essentially irreversible and that this coupling phenomenon can be disrupted by the high salt concentration in the elution buffer. Bead contacting time, in an analytical sense, denotes the time one hIgG molecule is in contact with a bead in a chromatographic column; therefore, it is the time a solute molecule has to interact with the bead either in a diffusive or convective mode. For example, at a linear velocity of 9.0 cm/min, t_b is calculated as 0.009 min, t_R is 0.55 min and, working with a ε_p of 0.9 [13,19], t_d is 7.7 min. Therefore, in 0.009 and 0.55 min a hIgG molecule can penetrate a bead radius of 13.55 and 107.15 μm, respectively, by diffusive transport. However, the fluorescent

Table 1
Calculated bead contacting and column residence times for the dynamic uptake of hIgG-FITC by LMCB at linear velocities of 1.1 and 9.0 cm/min, respectively

Superficial velocity (cm/min)	Bead contacting time (min)	Column residence time (min)	Predicted bead penetration (μm) when	
			$t_b = t_D$	$t_r = t_D$
1.1	0.0727	4.545	38.77	306.50
9.0	0.009	0.556	13.55	107.15
Column dimensions and parameters				
Radius of column (cm)	0.5			
Cross-sectional area of column (cm^2)	0.196			
Volume of beads (ml)	0.98			
Length of packed column (cm)	5.0			
Average bead radius* (R_p) (μm)	400			
Diffusion coefficient of hIgG** (D) (cm^2/s)	6.2×10^{-7}			
Calculated diffusion time[a] (min)	7.7			

Additionally, bead penetration distances, the distance a hIgG molecule can penetrate LMCB beads under purely diffusive conditions are also listed. The value of the diffusion coefficient for hIgG was taken from [17].

[a] $t_D = R_p^2 \varepsilon_p / 5D$, with $\varepsilon_p = 0.9$.

* Estimated by environmental SEM analysis and light microscopy.

** Taken from [17].

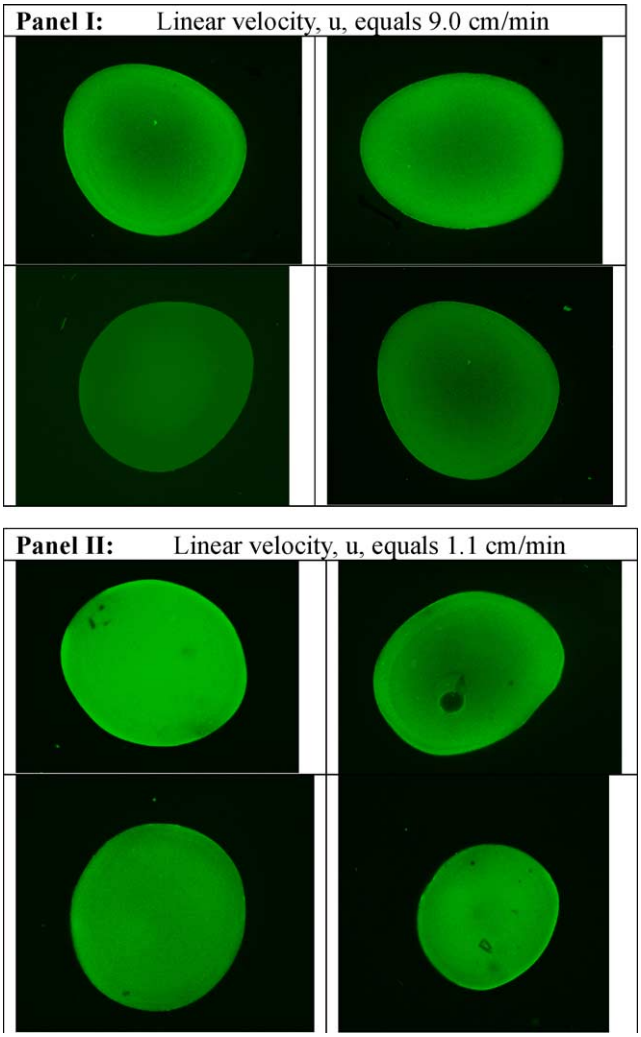

Fig. 8. Confocal images of sample beads obtained from dynamic uptake of hIgG to LMCB. Images were obtained for a protein solution feed of 10 mg/ml FITC-hIgG in binding buffer (10 mM KH_2PO_4, pH 6.0), which was continuously feed through an HR 5/5 column (3.5 cm × 0.5 cm) until the effluent concentration reached 90% of the feed concentration. Columns were run at linear velocities of 1.1 and 9.0 cm/min for each feed concentration. Images were obtained by taking a 25 μm deep z-section scan at the midpoint of the bead.

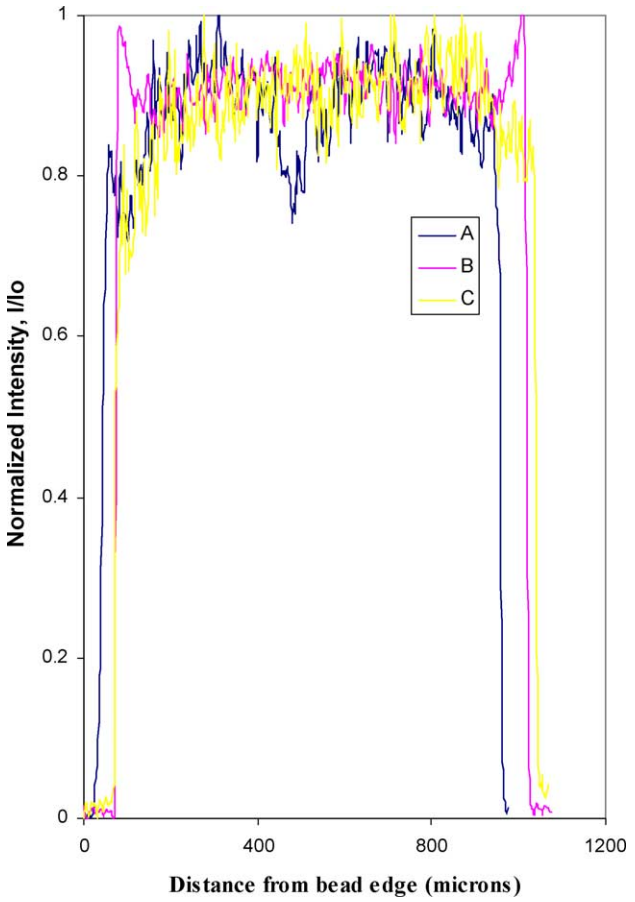

Fig. 9. Fluorescence intensity profile of the dynamic experiment at a feed concentration of 10 mg/ml FITC hIgG at a linear velocity of 1.1 cm/min. Column was fed continuously until the effluent concentration was 90% of the feed concentration, and then washed till the baseline dropped to zero. The beads were then sectioned and viewed under a confocal microscope. Three different beads were scanned and the three independent scans are shown in the Fig. 10. Normalized intensity profiles correspond to panel II in Fig. 8.

profiles for dynamic hIgG-FITC uptake to 90% saturation for a feed concentration of 10 mg/ml at a linear velocity of 9.0 cm/min, reveal that at the bead center, a bead radius of 400 μm, approximately 55–65% of the sites were occupied. Additionally, at a bead radius of 100 μm from the exterior, approximately 90% of the sites available were occupied. Thus, fluorescently tagged IgG molecules occupy sites that are not accessible through purely diffusive transport. The accelerated transport observed in this study can be best explained by a component of convective solute transport; however, the relative magnitude cannot be established at this point.

The analysis of mass transfer in these studies illustrates the argument that the mode of solute transport within the LMCB support is diffusion-convection in nature. This view is further demonstrated by a comparison of the batch and dynamic hIgG-FITC uptake experiments. Inspection of the intensity profiles for the 24 h batch experiment at a feed concentration of 10 mg/ml FITC-hIgG (Fig. 6) and the dynamic uptake profiles for a linear velocity of 9.0 cm/min (Fig. 10), show curves that look similar. This suggests that solute transport was partly governed by convective forces due to the fact that transport was not limited and the hIgG molecules had an opportunity to access all available binding sites.

In our continuing and future research efforts, we are undertaking the modeling of the profiles obtained in an attempt to estimate the effective diffusivity of proteins. Diffusivities will then be calculated from confocal images by first estimating the fractional uptake (η, where η equals $I_{(r)}/(I_{(\max@\, r=R)})$, based on the radial position of the adsorption front and then curve fitting the time-dependent fractional uptake data using the finite volume solution of the model [18]:

$$\frac{\varepsilon_p D_p C_o t}{R^2 Q_{\max}} = \frac{1}{2} - \frac{1}{3}(1-\eta^3) - \frac{1}{2}\eta^2,$$

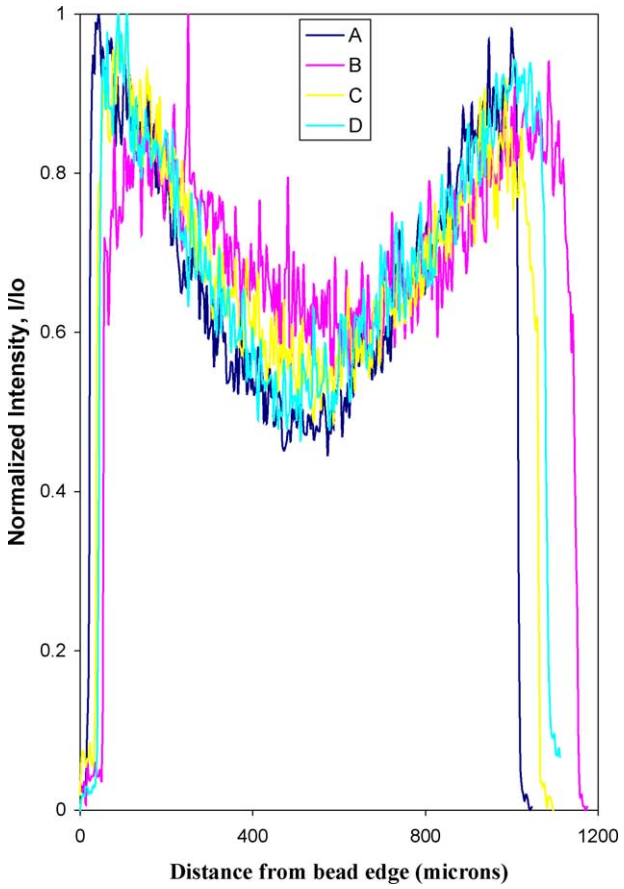

Fig. 10. Fluorescence intensity profile of the dynamic experiment at a feed concentration of 10 mg/ml FITC hIgG at a linear velocity of 9.0 cm/min. Column was fed continuously until the effluent concentration was 90% of the feed concentration, and then washed till the baseline dropped to zero. The beads were then sectioned and viewed under a confocal microscope. Four different beads were scanned and the four independent scans are shown in the Fig. 10. Normalized intensity profiles correspond to panel I in Fig. 8.

where η is the fractional uptake, ε_p is the intraparticle porosity, C_o is the hIgG feed concentration, R is the particle radius, and Q_{max} is the maximum static binding capacity. Finally, the parameters (number of transfer units (NTU)) that govern the solute transport and that are pertinent to scale-up will be evaluated by pulse-injection analysis and expressed as a function of linear velocity (u).

4. Conclusion

We have shown that the transport of biomolecules in matrices with open architecture is a combination of convective and diffusive fluxes. Thus, in theory, it is possible to design matrices with architecture that will promote convection in addition to diffusion of solute molecules. We believe that quantum leaps in the chromatographic performance of matrices employed in preparative bioseparations will result when advances in matrix preparation technology are coupled with novel designs to allow efficient utilization of mass transfer fluxes under a wide range of operating conditions.

References

[1] M. Leonard, J. Chromatogr. B 699 (1997) 3.
[2] D. Frey, E. Schweinheim, Cs. Horvath, Biotechnol. Prog. 9 (1993) 273.
[3] N. Afeyan, G. Mazsaroff, L. Varady, S. Fulton, Y. Yang, F. Regnier, J. Chromatogr. 519 (1990) 1.
[4] G. Carta, A. Rodrigues, Chem. Eng. Sci. 48 (23) (1993) 3927.
[5] D. Farnan, D. Frey, Cs. Horvath, Biotechnol. Prog. 13 (1997) 429.
[6] O. Larsson, E. Gustavsson, A. Axelsson, J. Mol. Recognit. 11 (1998) 270.
[7] A. Subramanian, K. Van Cott, D. Milbrath, W. Velander, J. Chromatogr. A 672 (1994) 11.
[8] H. Kim, M. Hayashi, K. Nakatani, N. Kitamura, Anal. Chem. 68 (3) (1996) 409.
[9] A. Ljunglof, J. Thommes, J. Chromatogr. A 813 (1998) 387.
[10] A. Ljunglof, R. Hjorth, J. Chromatogr. A 743 (1996) 75.
[11] S.R. Dziennik, E.B. Belcher, G.A. Barker, M.J. DeBergalis, S.E. Fernandez, A.M. Lenhoff, Am. Proc. Natl. Acad. Sci. U.S.A. 100 (2) (21 January 2003) 420.
[12] S.K. Roy, J.S. Todd, W.G. Glasser, US Patent 5,770,712.
[13] W. Collins, Sep. Purif. Methods 26 (2) (1997) 215.
[14] A. Subramanian, S. Roy, C. Mascoli, J. Hommerding, J. Liq. Chromatogr. 24 (17) (2004) 2649.
[15] A. Subramanian, J. Hommerding, J. Liq. Chromatogr. 24 (17) (2004) 2671.
[16] A. Rodrigues, A. Ramos, J. Loureiro, M. Diaz, Z. Lu, Chem. Eng. Sci. 47 (17 and 18) (1992) 4405.
[17] G. Skidmore, B. Horstmann, H. Chase, J. Chromatogr. 498 (1990) 113.
[18] W.K. Teo, D.M. Ruthven, Ind. Eng. Chem. Proc. Des. Dev. 25 (1986) 17.
[19] J.A. Kaster, W. de Oliveira, W. Glasser, W.H. Velander, J. Chromatogr. 648 (1993) 79.
[20] A.M. Clausen, P.W. Carr, Anal. Chem. 70 (1998) 378.